University of Baghdad
College of Engineering
JOURNAL OF ENGINEERING

Journal of Engineering

journal homepage: www.jcoeng.edu.iq

Volume 30 Number 8 August 2024

Performance of Serpentine Flow Solar Water Heater using Different Mass Flowrate

Ahmed Sarhan Abdulsitar [1,*], **Nofal Adrees Hasan** [2]

[1] Department of Mechanical Engineering, College of Engineering, Zakho University, Kurdistan Region, Iraq
[2] Department of Mechanical Engineering, College of Engineering, Mosul University, Mousl, Iraq

ABSTRACT

The utilization of Solar Water Heating Systems (SWHS) is a potential solution to use as an alternative to fuel and electricity in areas where these resources are scarce, costly, and not easily accessible. Research was conducted in Duhok City, Kurdistan of Iraq to evaluate the efficiency of a traditional type of SWHS, namely the serpentine collector variant. An active system collector that employed a moving water pump to facilitate the circulation of water inside the systems was used in the experiment. An analysis was conducted to assess the performance of the collector concerning solar irradiation, wind speed, and mass flow rate. This study utilized a Flat Plate Collector (FPC) with a tubular serpentine shape absorber made of steel sheet and copper tube. The serpentine collector had a maximum total heat loss coefficient of 5.53 W/m^2.℃. The serpentine collector demonstrated its highest level of practical heat gains at 561W. Its performance was observed to improve with increasing solar irradiation and water mass flow rate, but declined when wind speed exceeded the rated values. The serpentine collector achieved maximum efficiency with a flowrate of 0.042 kg/s, resulting in a productivity of 66.6%. While the maximum increase in water tank temperature in the serpentine collector was 25.8 ℃ at the mass flowrate 0.05 kg/s.

Keywords: Solar water heating system; Serpentine collector; Copper tube; Heating water; Storage temperature

1. INTRODUCTION

Renewable energy is a sustainable and environmentally friendly alternative to non-renewable energy sources. The widespread utilization of fossil fuels for water heating results in significant environmental harm **(Vengadesan and Senthil, 2020)**. Fuel is a significant contributor to air pollution and the release of greenhouse gases **(Al-Madani, 2006)**. Solar energy, a renewable energy source, offers various advantages in terms of electricity generation and even hot water production. Solar energy is considered one of the most favorable options among the existing renewable sources of clean energy due to its

*Corresponding author
Peer review under the responsibility of University of Baghdad.
https://doi.org/10.31026/j.eng.2024.08.02
This is an open access article under the CC BY 4 license (http://creativecommons.org/licenses/by/4.0/).
Article received: 16/07/2023
Article revised: 11/09/2023
Article accepted: 29/07/2024
Article published: 01/08/2024

widespread **(Khan et al., 2018)**. The abundant and uninterrupted availability of solar energy will effectively fulfill both present and future energy requirements **(Amori and Adeeb, 2016)**. In recent times, there has been a notable growth in the use of solar thermal collectors for both home and industrial purposes, mostly because of the substantial improvement in their efficiency **(Ahmed et al., 2017)**. The solar thermal collector is a crucial element in a solar thermal system, as it is responsible for efficiently converting sunlight into heat **(Nima and Ali, 2017)**. Results from a solar collector are affected by multiple parameters, such as the design, material of the collector, and local weather conditions **(Al-Najjar, 2015)**. According to **(Patel et al., 2012)**, hot water service appliances contribute to around 20% of overall residential energy usage. To tackle this problem, SWHS has been created, which harnesses solar radiation and transforms it into thermal energy to heat water. SWHS is an environmentally friendly, dependable, and economical approach to efficiently utilizing solar energy to meet 50-80% of hot water requirements **(Faisal Ahmed et al., 2021)**. Several methodologies have been suggested to enhance the efficacy of solar collectors **(Al-Dabbas et al., 2021; Padovan and Del Col, 2010; Al-Amayreh et al., 2020; Kumar et al., 2021)**. A FPC is a crucial equipment that enables the direct utilization of solar energy for water heating in both residential and industrial settings **(Verma et al., 2020)**. Numerous investigations have been conducted on FPCs, including **(Ibrahim et al., 2011**; **Tiwari et al., 2021; Cruz-Peragon et al., 2012; Bhowmik and Amin, 2017)**. As of the end of 2020, SWHS has been used in at least 134 countries worldwide, generating 501 GW of thermal energy **(Salim, 2020)**. The first solar collector was developed by De Saussure in 1767 in Switzerland, named "hotbox," **(Salim, 2020)**. In the absence of solar radiation, utilizing solar energy processes can present considerable challenges **(Saeed and Abdullah, 2022)**. SWHS might be direct or indirect system. Direct systems circulate water through a solar-exposed collector, while indirect systems employ a heat transfer fluid to transmit heat to a storage tank **(Jebaraj and Iniyan, 2006)**. Researchers strive to optimize the efficiency of solar water heaters by modifying the collector design and implementing phase change materials as an energy storage system **(Hamdoon and Ali, 2023).** The serpentine design optimizes the contact surface area with the fluid, resulting in enhanced heat transfer and greater thermal efficiency in comparison to conventional flat plate collectors. The improved heat transfer in these systems is additionally strengthened by the natural convection currents generated within the fluid, which can be augmented by careful design and positioning of the coils or tubes. The primary components of a standard panel consist of a black surface that is capable of absorbing incident solar radiation (typically composed of copper, aluminum, or steel), a transparent glazing cover that can transmit radiation to the absorber, internal channels that contain the heat transfer fluid, a structure that can protect the components and anchor them in place, and insulation that can reduce the heat losses of the collector. Two methods, active and passive systems, are commonly used to absorb solar heat. Active systems require a pump to circulate water in the system. In active systems, the collector is separate from the storage tank and the pump circulates water through the collector to absorb solar heat, which is then transferred to the storage tank. The efficiency of an active solar water heating system ranges from 35% to 80% **(Khalifa, 1998)**, superior to a passive system by 30–50% **(Nahar, 2002)**. In contrast, passive systems utilize natural convection to circulate water in the system, the heated water rises naturally to the storage tank due to the difference in density between the hot and cold water . **(Nasir, 2019)** conducted a practical experiment on affecting of mass flowrate on a FPC in Babylon, Iraq. Five different mass flowrate was used in the experiment that was (0.14, 0.21, 0.28, 0.35, and 0.42 kg/s. The plastic absorber used in the experiment with a length of 17.4 m, the glass

thickness was 3.5 mm, and the area of the collector was 2.4 m^2. The results showed that the system achieved the highest efficiency with 0.35 kg/s mass flowrate. FPCs are often built for hot water systems with operating temperatures ranging from 40 to 60°C **(Nasir, 2019)**. Constant advancements in size reduction and improved efficiency are driving the popularity of FPCs for low and medium-heating applications **(Pandey and Chaurasiya, 2017)**. The efficiency of the collector decreases with an increase in water temperature **(Abdulsitar and Hasan, 2022)**. **(Çomakli et al., 2012)** stated that it is necessary to optimize the area of the FPC and the size of the storage tank. They found that a storage tank to FPC area ratio of 50-70 L/m2 is ideal. **(Ahmed, 2016)** performed an empirical investigation on the effect of dust on the glass of the FPC. The study found that system efficiency decreased with dusty glass, and the FPC's glass must be cleaned regularly to maintain high performance. **(Sidky et al., 2019)** conducted an experimental study using harp, spiral, and serpentine absorber collectors. The collector area was 0.1 m^2. The serpentine collector provided the highest efficiency and saved the most energy, while the spiral collector was better than the harp collector. **(Bakari et al., 2014)** performed an empirical investigation on the effect of glass thickness on FPC. Four different glass thicknesses wereused that was 3mm, 4mm, 5mm, and 6 mm. The study found that 4mm thickness provided the maximum efficiency, while the minimum efficiency was achieved with 6mm glass thickness. The popularity of SWHS is increasing globally, with various types of systems available to meet different needs and preferences.

The aim of the present paper is to know the effect of the water mass flow rate on the thermal efficiency of the serpentine collector. The experiment was conducted in Dohuk city in Iraq. Iraqi peoples suffer from a lack of hot water in the winter, the solar collector is a good alternative to electricity and fuel. The active system was used in the experiment, the DC pump was used to circulate the water inside the system, and steel was used as a collector with an area of 1 m^2.

2. THEORETICAL BACKGROUND OF HEAT TRANSFER IN RELATION TO SOLAR COLLECTORS

2.1. The Heat Energy Balance Equation of the Flat Plate Collector

The FPC collects solar radiation and converts it into thermal energy, as illustrated in **Fig.1**. The amount of heat energy produced by the FPC, denoted as Q_i, can be measured using Eq**.** (1).

$$Q_i = IA \tag{1}$$

Eq. (2) is used to calculate the amount of heat energy produced by an FPC, takes into account the solar irradiance (I) and the surface collector area (A). However, not all solar radiation that reaches the plate is transmitted through the glass cover, and the absorber plate may not absorb all of the heat. To account for this, the transmittance (τ) of the glass cover is equal to 0.89 and the absorptivity (α) of the plate is equal to 0.81 are added to Eq**.** (2). where the value of τ = 0.89 based on the collector's thickness and angle of the glass while α = 0.81 based on the plate's material and color.

$$Q_i = (\tau\alpha)\, IA \tag{2}$$

When the absorber plate of the FPC is hotter than the surrounding temperature, some of the solar radiation is reflected, causing heat loss (Q_o) from the FPC to the surroundings. The heat

loss can be determined by utilizing Eq. (3), which U_L represents the total heat coefficient, (Tp) denotes the plate temperature, and (Ta) signifies the ambient temperature.

$$Q_o = U_L A(Tp - Ta) \tag{3}$$

After calculating Qi and Qo, the useful heat of the collector (Q_U) can be determined. This represents the amount of heat energy that is available for use or storage. Q_U can be calculated using Eq. (4). **(Ahmed, 2016)**.

$$Q_U = (\tau\alpha)\, IA - U_L A(Tp - Ta) \tag{4}$$

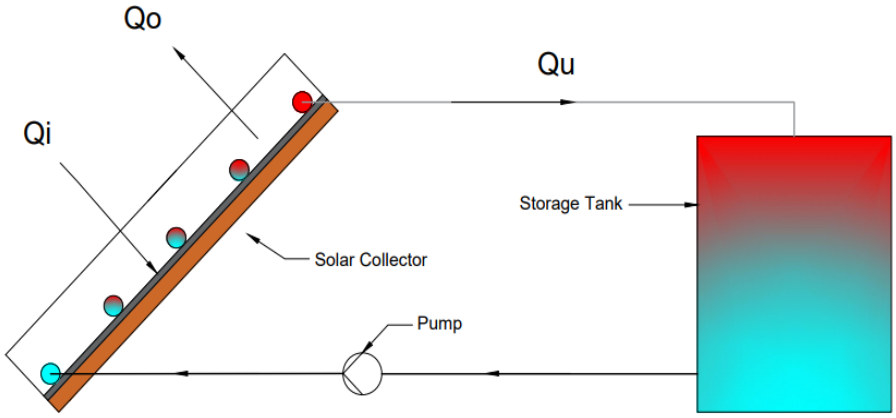

Figure 1. Schematic drawing

To assess the efficiency of a collector, the standard approach involves subjecting the collector to solar radiation and monitoring the temperatures of the fluid at the intake and output, as well as the rate at which the fluid flows **(Farhan and Sahi, 2017)**. Q_u can be estimated using the working fluid's thermal energy as it flows through the collector **(Ahmed, 2016)**.

$$Q_u = \dot{m} C_p (To - Ti) \tag{5}$$

Where To is the fluid outlet temperature and Ti is the fluid inlet temperature, and $\dot{m}$ is the mass flow rate and C_p is the specific heat capacity. Eq. (6) states that the heat removal factor is a ratio of $Q_u$to Q_U, also known as the Hottel-Whillier Equation.

$$F_R = \frac{\dot{m} C_p (T_o - T_i)}{(\tau\alpha)\, IA \; - U_L A(Ti - Ta)} \tag{6}$$

Eq. (7) can be used to get the collector's thermal efficiency.

$$\eta = \frac{\int Q_u \, dt}{\int Q_i \; dt}$$

$$\eta = F_R \tau\alpha - F_R U_L \left(\frac{T_i - T_a}{I}\right) \tag{7}$$

Whete U_L is overall heat transfer coefficient and can be calculated by using Eq. (8).

$$U_L = U_T + U_B + U_E \tag{8}$$

Where U_T is top loss coefficient, U_B is bottom loss coefficient, and U_E edge loss coefficient.

2.2.1 Top loss coefficient (U_T)

U_t can be calculated by using Eq. (9) **(Tiwari et al., 2016)**

$$U_t = \left[\frac{1}{h_1 + h_2} + \frac{1}{h_3 + h_4} + \frac{1}{h_5}\right]^{-1} \quad (9)$$

Where h_1 heat lost through convection from the glass to the surrounding air and can be calculated by using Eq. (10).

$$h_1 = 2.8 + 3V \quad (10)$$

Where V is air velocity

Calculations can be made for the radiation heat loss from glass to the surrounding air by using Eq. (11)

$$h_2 = \varepsilon_g \sigma \frac{[(T_g + 273)^4 - (T_{sky} + 273)^4]}{T_g - T_a} \quad (11)$$

The glass temperature is T_g, and the sky temperature is T_{sky}, where ε_g is the glass emissivity coefficient and σ is Stefan's constant (σ = 5.67 $\times 10^{-8}$ W/m^2K^4), while $T_{sky} = T_a - 6$.

Eq. (12) can be used to compute the heat losses via convection from the absorber plate to the glass cover.

$$h_3 = \frac{N_u k_{ab}}{d} \quad (12)$$

Where k_{ab} is the air gap thermal conductivity while (d) is the air gap distance.
The Nusselt number of the air gap, denoted as N_u, can be determined by utilizing Eq. (13).

$$N_u = 1 + 1.44\left[1 - \frac{1708}{R_a cos\beta}\right]^{+}\left(1 - \frac{\sin(1.8\beta)^{1.6} \times 1708}{R_a cos\beta}\right) + \left[\left\{\frac{R_a cos\beta}{5830}\right\}^{\frac{1}{3}} - 1\right]^{+} \quad (13)$$

Where R_a is the Rayleigh number and can be calculated by using Eq. (14), while β is the collector angle inclination. The variable (g) represents the acceleration of gravity, ΔT represents the temperature differential between the plate and glass, υ represents the kinematic viscosity, and α_a represents the thermal diffusivity.

$$R_a = \frac{g\acute{\beta}\Delta T d^3}{\upsilon \alpha_a} \quad (14)$$

$$\acute{\beta} = \frac{2}{(T_p + T_g)} \quad (15)$$

The heat loss from the absorber plate to the glass cover by radiation can be calculated by using Eq. (16).

$$h_4 = \varepsilon_{eff}\sigma \frac{[(T_p + 273)^4 - (T_g + 273)^4]}{T_p - T_g} \quad (16)$$

Where ε_{eff} is the effective emissivity of the absorber plate and glass cover, and can be calculated by using Eq. (17). ε_p and ε_g are the effective emissivity of the plate and the effective emissivity of the glass, respectively.

$$\varepsilon_{eff} = \left[\frac{1}{\varepsilon_p} + \frac{1}{\varepsilon_g} - 1\right]^{-1} \quad (17)$$

The heat loss from glass to the ambient by the heat conduction can be calculated by using Eq. (18). k_g is the thermal conductivity of the glass and L_g is the thickness of the glass.

$$h_5 = \frac{k_g}{L_g} \quad (18)$$

2.2.2 Bottom Loss Coefficient (U_B)

Eq. (19) can be used to calculate the bottom loss coefficient **(Tiwari et al., 2016)**.

$$U_b = \left[\frac{1}{h7} + \frac{1}{h1 + h6}\right]^{-1} \quad (19)$$

$h6$ is the heat loss from the plate to the ambient through the insulation by heat radiation can be calculated by using Eq. (20). ε_i is the insulation emissivity.

$$h_6 = \varepsilon_i\sigma \frac{[(T_i + 273)^4 - (T_{sky} + 273)^4]}{T_i - T_a} \quad (20)$$

h_7 is the heat loss by the heat conduction through the insulation can be calculated by using Eq. (21). k_i represents the insulation thermal conductivity and L_i represents the insulation thickness.

$$h_7 = \frac{k_i}{L_i} \quad (21)$$

2.2.3 Edge Loss Coefficient (U_E)

The heat loss through the edge of the collector can be calculated by using Eq. (22). A_e represents the the area of the collector edge and A represents collector area **(Tiwari et al., 2016)**.

$$U_E = U_b\left(\frac{A_e}{A}\right) \quad (22)$$

3. MATERIALS AND METHODS

The copper tubing used to form the serpentine collector was challenging due to its complex shape. Consequently, the tubing was manufactured in Duhok's industrial workshops. The experiments were conducted in Duhok City across various days throughout 2022. The collector's data was collected using a data logger under varying weather conditions. As per Duhok's latitude, The collector was installed at an angle of 37° in the south direction, as illustrated in **Fig.2**. For the purposes of this study, the serpentine collector was examined. The collector was constructed using a copper tube, which was painted black, along with a plate, as shown in **Fig.3**. Copper was selected due to its ease of bending compared to steel and its better thermal conductivity than steel tubes.

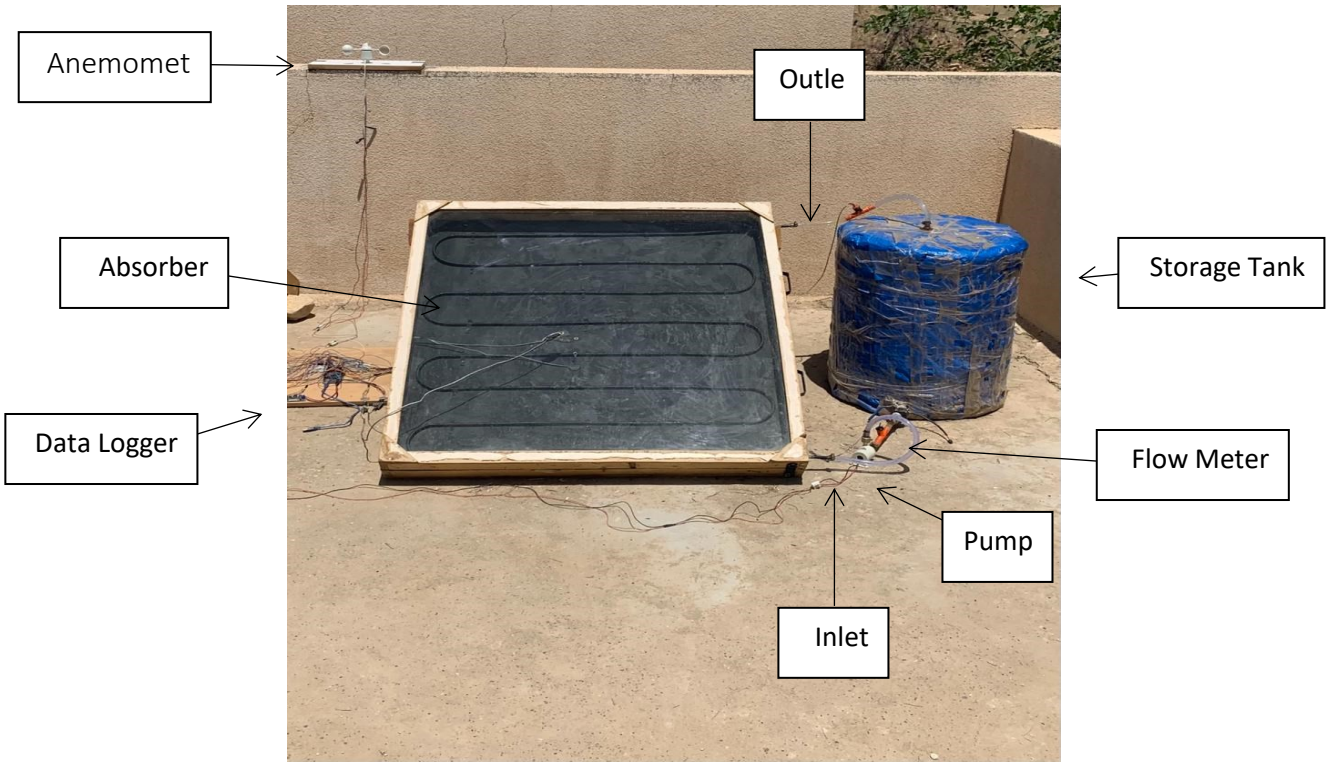

Figure 2. Experimental setup.

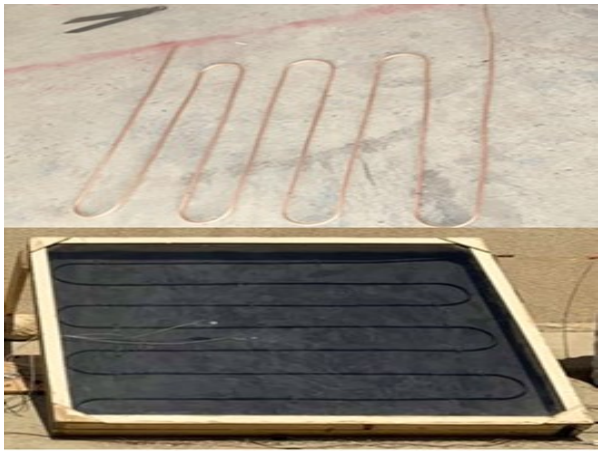

Figure 3. Serpentine collectors.

The copper tube had a thickness of 0.71 mm, which was deemed suitable for bending. **Table 1** shows the collector properties. The heated water collected by the solar collector was stored in an insulated tank with a capacity of 60 liters, as shown in **Fig.4**.

Table 1. Collector properties.

Item	Dimension	Material
Area of plate	1 m^2	Galvanized steel
Tube outer diameter	9.52 mm	Copper
Tube length	7.8 m	
Air gap Distance between tube	8.5 cm 11 cm	
Cover thickness	4 mm	Glass
Insulation thickness	2 cm	Wood

Figure 4. Insulated Storage tank.

Water entered the serpentine collector from the bottom and exited from the top, as illustrated in **Fig.5**. K-Type thermocouples were used to measure the temperatures of the plate, glass cover, and air gap. The Waterproof Ds18B20 temperature sensors were used to measure the water temperature. Temperature Sensor LM35 and a thermometer were employed to measure the ambient temperature. Additionally, a flow meter sensor was used to measure the water flow rate. In order to log and record the data collected throughout the experiment, an Arduino Mega microcontroller was utilized as a data logger.

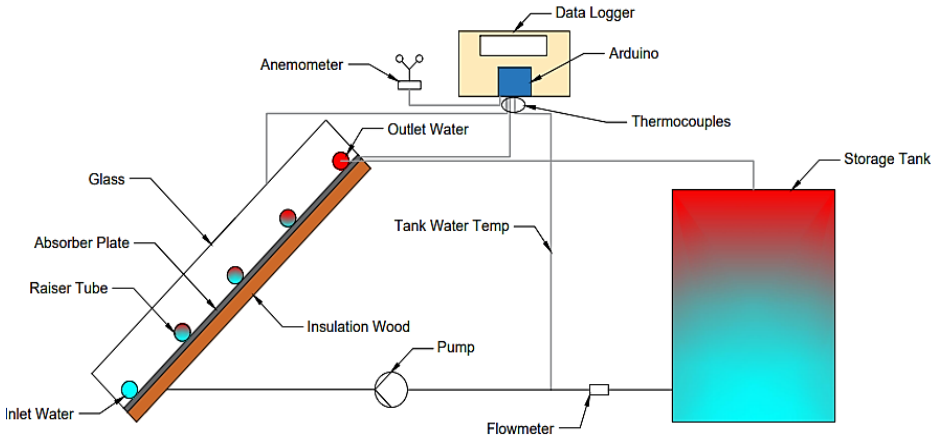

Figure 5. Sketch diagram of the solar water heater.

The SM206 device was used to measure the solar irradiance capable of measuring within a range of 1-3999 W and was installed on top of the collector, as illustrated in **Fig.6** that was installed at the same angle as the collector, as recommended by **(Yassen et al., 2019)**.

Figure 6. Solar power meter.

Wind speed was also measured during the experiment using two anemometers. The WH-SP-WS01 anemometer was used, as shown in **Fig.7**, along with the more accurate HP-866B digital anemometer

Figure 7. Wind speed meter.

4. UNCERTAINTY ANALYSIS

Uncertainty analysis can be used to assess the accuracy of the experiment **(Noghrehabadi et al., 2018)**. It is important to note that all devices used in the experiment have some degree of error in their measurements as shown in **Table 2**. To calculate the uncertainty of the collector efficiency, Eq. (7) was utilized, which includes all of the relevant variables, including the mass flow rate $(\dot{m})$, irradiance angle (W_S), temperature difference (ΔT), and solar irradiance (I) **(Noghrehabadi et al., 2016)**.

$$\omega_\eta = \left[\left(\frac{\Delta \dot{m}}{\dot{m}}\right)^2 + \left(\frac{\Delta W_S}{W_S}\right)^2 + \left(\frac{\Delta (T_o - T_i)}{(T_o - T_i)}\right)^2 + \left(\frac{\Delta I}{I}\right)^2\right]^{\frac{1}{2}} \quad (23)$$

$$\omega_\eta = [(0.01)^2 + (0.05)^2 + (0.005)^2 + (0.05)^2]^{\frac{1}{2}}$$

$$\omega_\eta = [0.005125]^{\frac{1}{2}}$$

$$\omega_\eta = 0.0716$$

$$\omega_\eta = 7.16\%$$

Table 2. The error rate of measurement equipment.

Measurement equipment	Error rate
Water mass flowrate sensor	±1%
Anemometer	±5%
Solar irradiance	±5%
Thermocouples	±0.5%

5. RESULTS AND DISCUSSION

Matlab program was employed to solve the equations of the solar collector. Data was recorded in June and July using 6 different water mass flow rates and all this data will be presented with showing the influence of solar irradiance, wind speed, and ambient temperature on the collector performance. **Fig.8** depicts the temperature of the inlet and outlet water tanks of the serpentine collector. As expected, the temperature increased with solar irradiance. **Fig.9** Shows the effect of water flow rate on the temperature of a solar water heater tank after 6 hours, The water tank temperature in the serpentine collectors reached its highest value at a flow rate of 0.05 kg/s. Overall, the performance of the serpentine collector was good across all flow rate values.

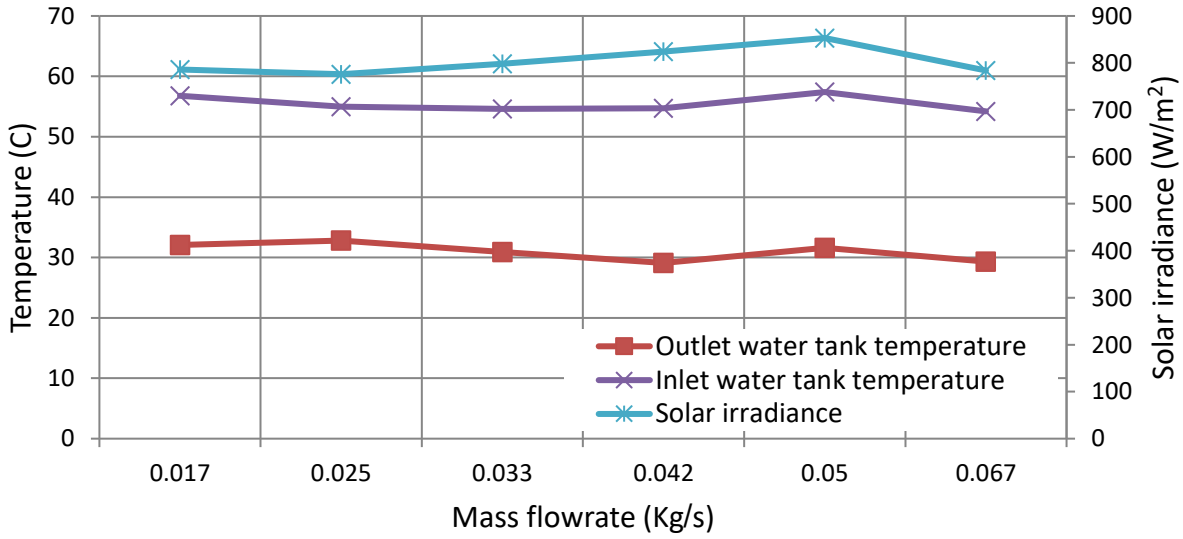

Figure 8. The effect of solar radiation on the temperature of a solar water heater tank.

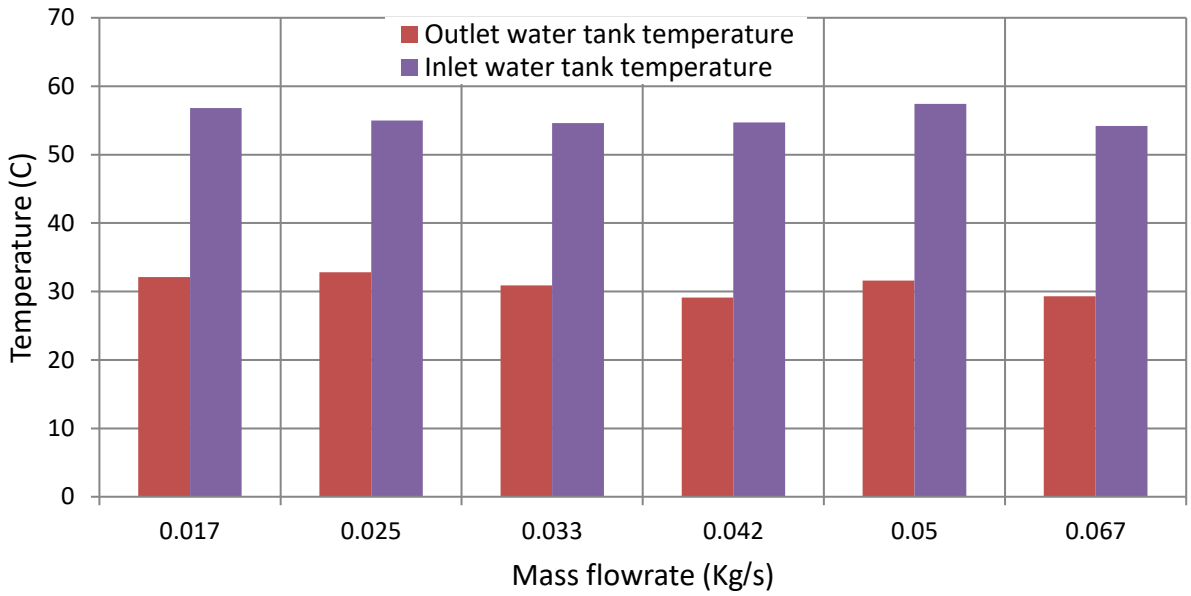

Figure 9. The effect of water flow rate on the temperature of a solar water heater tank.

Fig.10 demonstrates the correlation between temperatures of the glass cover, plate absorber, air gap, and ambient temperature with changes in mass flow rate and solar irradiance. The temperature of the glass cover and plate absorber increased with increasing solar radiation. The glass cover, plate absorber, and air gap temperatures reach their highest values at a flow rate of 0.05 kg/s. The ambient temperature reaches its highest value 38.6°C. Overall, these results indicate that the serpentine collector is effective at capturing and converting solar radiation into thermal energy.

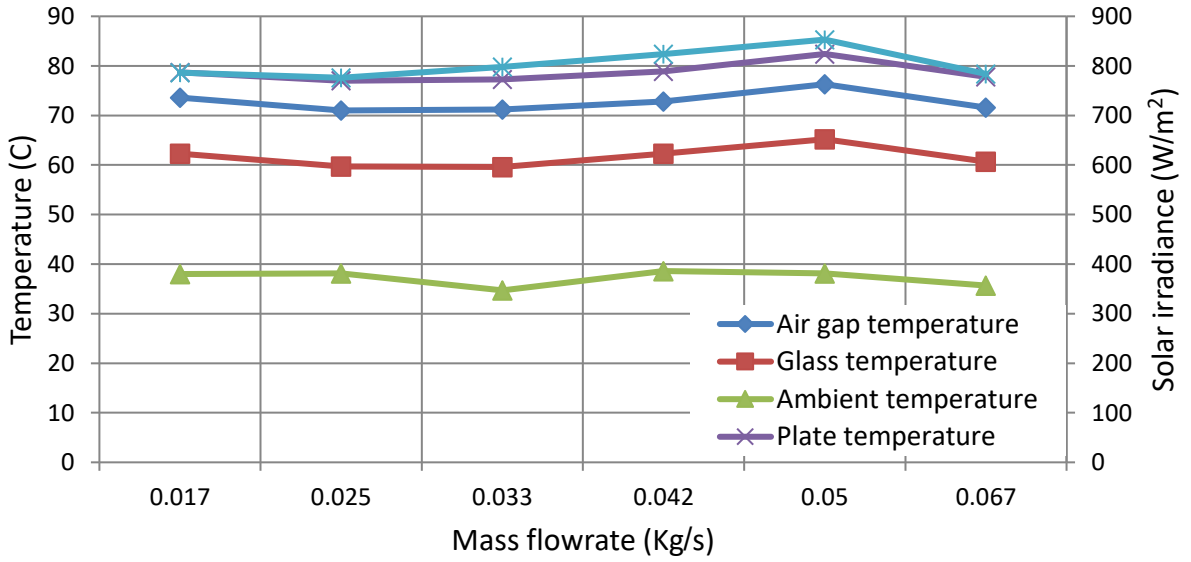

Figure 10. The impact of solar radiation and flow rate on the collector temperature.

Fig.11 illustrates the correlation between wind speed and the overall heat loss coefficient. As the velocity of the wind increases, the rate at which heat is transferred from the collector to the surrounding air is increased, resulting in an elevation of the overall coefficient of heat

loss. The findings indicated that the maximum overall heat loss coefficient was 5.31 W/m²°C when the wind speed was 1.1 m/s and the mass flow rate was 0.025 kg/s. These results demonstrate that wind speed significantly influences the overall heat loss coefficient of the serpentine collector.

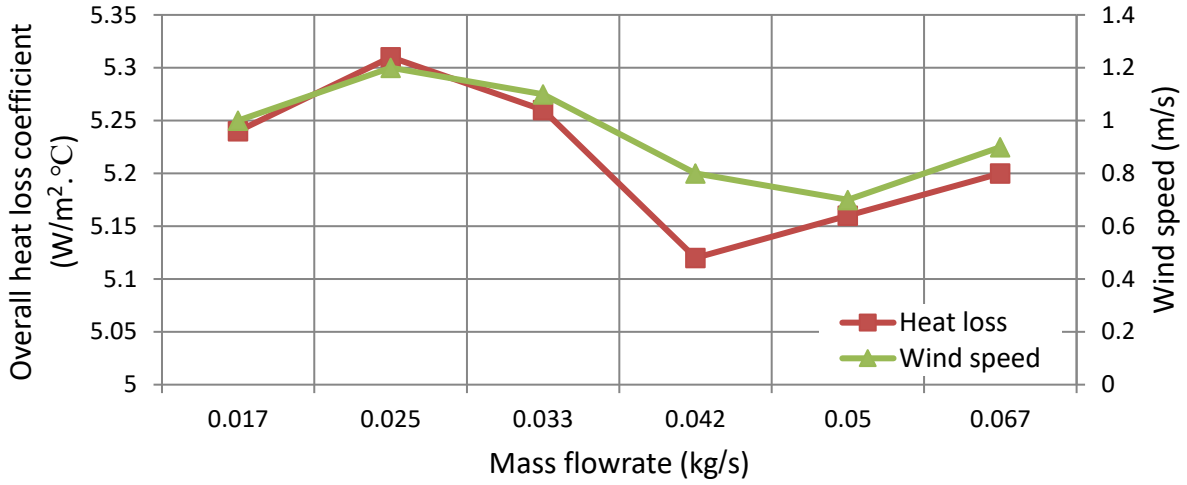

Figure 11. The effect of wind speed on the thermal performance of a solar thermal collector.

The useful heat gain of the serpentine collector is presented in **Fig. 12**. In general, the effective heat gain performance was good at any mass flow rate. The highest useful heat gain was obtained at 0.067 kg/s mass flow rate which shows that higher mass flow rates contribute to more accompanying with the experiment results. In **Fig. 13**, the efficiency of the serpentine collector is modified and made functional to the mass flow rate as well as solar irradiance. The serpentine collector, in general, was effective at all mass flow rates. The serpentine collector demonstrated superior efficiency compared to all other mass flow rate values, particularly at a mass flow rate of 0.042 kg/s; This shows that the mass flow rate should be properly chosen, to optimize efficiency.

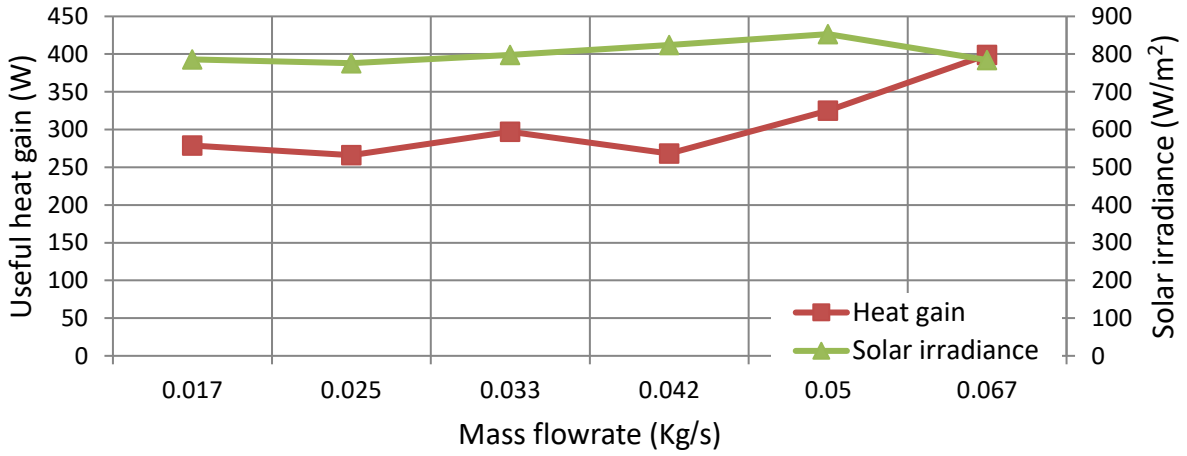

Figure 12. The effect of solar radiation and water flow rate on the heat output of a solar collector.

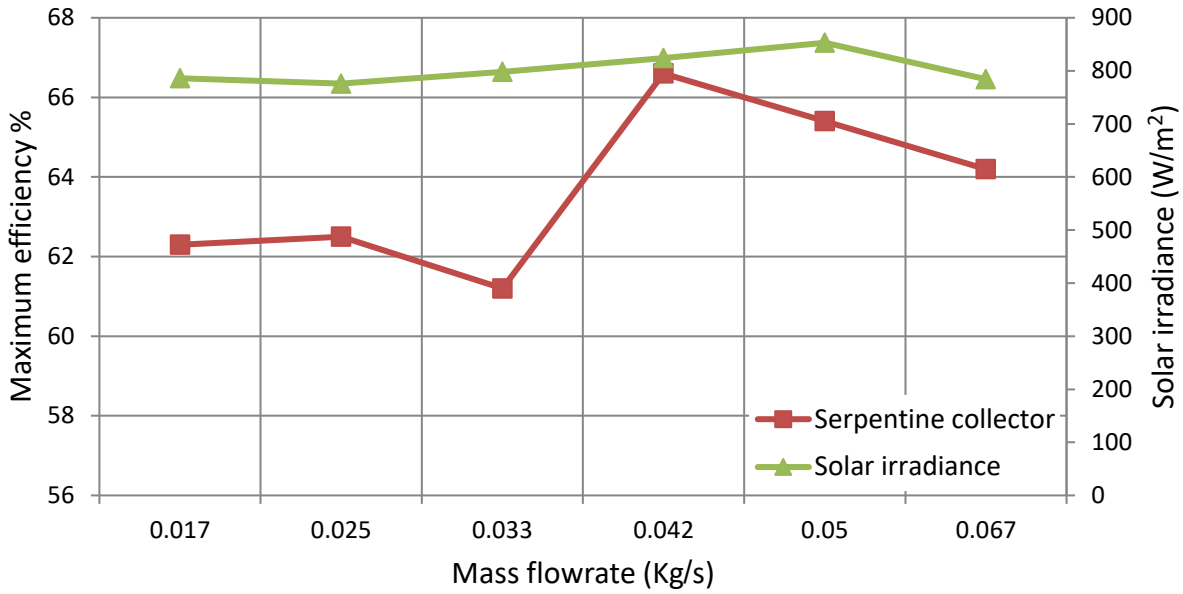

Figure 13. The optimal sun irradiance and water flow rate for solar collector efficiency.

6. CONCLUSIONS

The serpentine collector provided good performance, the collector performance was improved with increasing value of solar irradiance. Overall, results suggest that optimizing the design and operation of the serpentine collector can lead to improved performance and that careful consideration of variables such as solar irradiance, wind speed, and mass flow rate is important in achieving efficient and effective energy conversion.

The following key points can be concluded from the results:

- The serpentine collector achieved maximum efficiency of 66.6% at a flow rate of 0.042 kg/s.
- The highest increase in water tank temperature was observed at a mass flow rate of 0.05 kg/s, with a temperature increase of 25.8 ℃.
- The maximum useful heat gains were observed at a mass flow rate of 0.067 kg/s, with a value of 561 W.
- Wind speed had a negative impact on the thermal collector efficiency, with increasing wind speed leading to increased heat loss coefficient and decreased efficiency.
- The maximum overall heat loss coefficient was observed at a mass flow rate of 0.025 kg/s, with a value of 5.31 W/m^2℃.
- Errors in the results may have arisen due to limitations in measurements and devices.
- Thermal collector efficiency increased with increasing solar irradiance.
- Thermal collector efficiency decreased with increasing water tank temperature.

NOMENCLATURE

Symbol	Description	Symbol	Description
A	Area, m^2.	R_a	Rayleigh number.
C_p	Specific heat capacity, J/kg °C.	SWHS	Solar Water Heating System
F_R	Heat removal factor.	T	Temperature, °C.
FPC	Flat Plate Collector	U	Heat loss coefficient, W/m^2 °C.
h	Heat transfer coefficient, W/m^2 °C.	V	Velocity, m/s.
I	Solar irradiance, W/m^2.	α	Absorptivity
k	Thermal conductivity, W/m °C.	β	Collector angle inclination
ṁ	Mass flow rate, kg/s.	ε	Effective emissivity
N_u	Nusselt number.	τ	Transmittance
Q	Heat transfer, W.		

Acknowledgements

The authors thank the cooperation of the University of Zakho and the University of Mosul for conducting this research.

Credit Authorship Contribution Statement

Ahmed Abdulsitar: Analysis and writing of original manuscript.
Nofal Hasan: Conceptualization, Methodology, and Supervising.

Declaration of Competing Interest

The authors have no financial or personal relationships that could inappropriately influence this paper.

REFERENCES

Abdulsitar, A. S., and Hasan, N. A. 2022. Comparison between spiral and serpentine flow solar water heater. *Journal of University of Babylon for Engineering Sciences*, pp. 89–99.

Ahmed, O.K., 2016. Effect of dust on the performance of solar water collectors in Iraq. *International Journal of Renewable Energy Development*, pp. 65–72. https://doi.org/10.14710/ijred.5.1.65-72

Ahmed, S.F., Khalid, M., Rashmi, W., Chan, A., Shahbaz, K., 2017. Recent progress in solar thermal energy storage using nanomaterials. *Renewable and Sustainable Energy Reviews*, pp. 450–460. https://doi.org/10.1016/j.rser.2016.09.034

Al-Amayreh, M.I., Alahmer, A., Manasrah, A., 2020. A novel parabolic solar dish design for a hybrid solar lighting-thermal applications. *Energy Reports,* pp. 1136–1143.

Al-Dabbas, M., Alahmer, A., Mamkagh, A., Gomaa, M.R., 2021. Productivity enhancement of the solar still by using water cooled finned condensing pipe. D*esalination and Water Treatment,* 213, pp. 35–43. https://doi.org/10.5004/dwt.2021.26711

Al-Madani, H., 2006. The performance of a cylindrical solar water heater. *Renewable Energy*, pp. 1751–1763. https://doi.org/10.1016/j.renene.2005.09.010

Al-Najjar, H.M.T., 2015. Study of energy gains by orientation of solar collectors in Baghdad city. *Journal of Engineering,* 21(10), pp. 17–35. https://doi.org/10.31026/j.eng.2015.10.02

Amori, K.I., Adeeb, R.A., 2016. Absorber diameter effect on the thermal performance of solar steam generator. *Journal of Engineering,* 22(4), pp. 127–146. https://doi.org/10.31026/j.eng.2016.04.09

Bakari, R., Minja, R.J.A., Njau, K.N., 2014. Effect of glass thickness on performance of flat plate solar collectors for fruits drying. *Journal of Energy,* 2014(1), p.247287. https://doi.org/10.1155/2014/247287

Bhowmik, H., Amin, R., 2017. Efficiency improvement of flat plate solar collector using reflector. *Energy Reports 3*, pp. 119–123. https://doi.org/10.1016/j.egyr.2017.08.002

Çomakli, K., Çakir, U., Kaya, M., Bakirci, K., 2012. The relation of collector and storage tank size in solar heating systems. *Energy Conversion and Management,* pp. 112–117. https://doi.org/10.1016/j.enconman.2012.01.031

Cruz-Peragon, F., Palomar, J.M., Casanova, P.J., Dorado, M.P., Manzano-Agugliaro, F., 2012. Characterization of solar flat plate collectors. *Renewable and Sustainable Energy Reviews,* pp. 1709–1720. https://doi.org/https://doi.org/10.1016/j.rser.2011.11.025

Faisal Ahmed, S., Khalid, M., Vaka, M., Walvekar, R., Numan, A., Khaliq Rasheed, A., Mujawar Mubarak, N., 2021. Recent progress in solar water heaters and solar collectors: A comprehensive review. *Thermal Science and Engineering Progress,* 100981. https://doi.org/10.1016/j.tsep.2021.100981

Farhan, A.A., Sahi, H.A., 2017. Energy analysis of solar collector with perforated absorber plate. *Journal of Engineering,* 23(9), pp. 89–102. https://doi.org/10.31026/j.eng.2017.09.07

Hamdoon, O.M., Ali, I.A., 2023. The experimental investigation of double-pass solar air heater with V-corrugated plate, Phase-Change Material and Baffles Under Recycling Operation. *Al-Rafidain Engineering Journal,* pp. 256–271.

Ibrahim, A., Othman, M.Y., Ruslan, M.H., Mat, S., Sopian, K., 2011. Recent advances in flat plate photovoltaic/thermal (PV/T) solar collectors. *Renewable and Sustainable Energy Reviews,* pp. 352–365. https://doi.org/10.1016/j.rser.2010.09.024

Jebaraj, S., Iniyan, S., 2006. A review of energy models. R*enewable and Sustainable Energy Reviews,* pp. 281–311.

Khalifa, A.-J.N., 1998. Forced versus natural circulation solar water heaters: A comparative performance study. *Renewable Energy,* pp. 77–82.

Khan, M.M.A., Ibrahim, N.I., Mahbubul, I.M., Muhammad. Ali, H., Saidur, R., Al-Sulaiman, F.A., 2018. Evaluation of solar collector designs with integrated latent heat thermal energy storage: A review. *Solar Energy,* pp. 334–350. https://doi.org/10.1016/j.solener.2018.03.014

Kumar, P.M., Sudarvizhi, D., Prakash, K.B., Anupradeepa, A.M., Raj, S.B., Shanmathi, S., Sumithra, K., Surya, S., 2021. Investigating a single slope solar still with a nano-phase change material. *Materials Today: Proceedings,* pp. 7922–7925.

Nahar, N.M., 2002. Capital cost and economic viability of thermosyphonic solar water heaters manufactured from alternate materials in India. *Renewable Energy,* pp. 623–635.

Nasir, K.F., 2019. Thermal performance of plastic receiver in solar collector. *Journal of Engineering,* 25(7), pp. 37–60. https://doi.org/10.31026/j.eng.2019.07.03

Nima, M.A., Ali, A.M., 2017. Numerical study of heat transfer enhancement for a flat plate solar collector by adding metal foam blocks. *Journal of Engineering,* 23(12), pp. 13–32. https://doi.org/10.31026/j.eng.2017.12.02

Noghrehabadi, A., Hajidavaloo, E., Moravej, M., 2016. Experimental investigation of efficiency of square flat-plate solar collector using SiO2/water nanofluid. *Case Studies in Thermal Engineering,* pp. 378–386. https://doi.org/10.1016/j.csite.2016.08.006

Noghrehabadi, A., Hajidavaloo, E., Moravej, M., Esmailinasab, A., 2018. An experimental study of the thermal performance of the square and rhombic solar collectors. *Thermal Science,* pp. 487–494. https://doi.org/10.2298/TSCI151228252N

Padovan, A., Del Col, D., 2010. Measurement and modeling of solar irradiance components on horizontal and tilted planes. *Solar Energy,* pp. 2068–2084. https://doi.org/https://doi.org/10.1016/j.solener.2010.09.009

Pandey, K.M., Chaurasiya, R., 2017. A review on analysis and development of solar flat plate collector. *Renewable and Sustainable Energy Reviews,* pp. 641–650. https://doi.org/10.1016/j.rser.2016.09.078

Patel, K., Patel, P., Patel, J., 2012. Review of solar water heating systems. *International Journal of Advanced Engineering Technology*, pp. 146–149.

Saeed, D.N. and Abdullah, A.Y., 2022. Investigation of air solar collector with energy storage for domestic purposes. *Academic Journal of Nawroz University,* 11(3), pp.193-201. https://doi.org/10.25007/ajnu.v11n3a1370

Salim, R. D., 2020. Design and improving the work of a concave solar collector-CSC. *Periodicals of Engineering and Natural Sciences*, pp. 1471–1481.

Sidky, M. B., Haroun, K., Shukri, N., & Yacoob, K. (2019). Performance study of different types of solar water- heaters collectors. *Applications of Modelling and Simulation*, pp. 179–187. http://arqiipubl.com/ams

Tiwari, A.K., Gupta, S., Joshi, A.K., Raval, F., Sojitra, M., 2021. TRNSYS simulation of flat plate solar collector based water heating system in Indian climatic condition. *Materials Today: Proceedings*, pp. 5360–5365. https://doi.org/10.1016/j.matpr.2020.08.794

Tiwari, G. N., Tiwari, A., & Shyam. 2016. Solar water-heating systems. in: Handbook of solar energy. *Energy Systems in Electrical Engineering. Springer, Singapore.* https://doi.org/10.1007/978-981-10-0807-8_8

Vengadesan, E., Senthil, R., 2020. A review on recent development of thermal performance enhancement methods of flat plate solar water heater. *Solar Energy,* pp. 935–961.

Verma, S.K., Sharma, K., Gupta, N.K., Soni, P., Upadhyay, N., 2020. Performance comparison of innovative spiral shaped solar collector design with conventional flat plate solar collector. *Energy,* P. 194. https://doi.org/10.1016/j.energy.2019.116853

Yassen, T.A., Mokhlif, N.D., Eleiwi, M.A., 2019. Performance investigation of an integrated solar water heater with corrugated absorber surface for domestic use. *Renewable Energy,* pp. 852–860. https://doi.org/10.1016/j.renene.2019.01.114

أداء سخان المياه الشمسي ذو التدفق المعوج باستخدام معدل تدفق كتلة مختلفة

أحمد سرحان عبدالستار[1]، [*], نوفل ادريس حسن[2]

[1] قسم الهندسة الميكانيكية ، كلية الهندسة ، جامعة زاخو ، إقليم كوردستان، العراق

[2] قسم الهندسة الميكانيكية ، كلية الهندسة ، جامعة الموصل ، الموصل، العراق

الخلاصة

تعتبر أنظمة تسخين المياه بالطاقة الشمسية طريقة بديلة لتسخين المياه ، خاصة في المناطق التي يكون فيها الوقود والكهرباء باهظين أو من يصعب الوصول إليهما. في هذه الدراسة أجريت تجربة في مدينة دهوك بكردستان العراق لتقييم أداء جامع اعوج وهو أحد أنواع أنظمة تسخين المياه بالطاقة الشمسية. كان المجمع المستخدم في التجربة عبارة عن نظام نشط يستخدم مضخة مياه لتدوير المياه في النظام. تم تحليل أداء المجمع بناءً على المتغيرات التالية: الإشعاع الشمسي وسرعة الرياح ومعدل تدفق الكتلة. كان المجمع المستخدم في التجربة عبارة عن مجمّع صفيح مسطح بامتصاص شكل المعوج ، والذي يستخدم صفيحة فولاذية وأنبوب نحاسي ، ومع ذلك ، تم تركيب المجمع بزاوية ٣٧ درجة في الاتجاه الجنوب. تم تقييم أداء مجمّع السربنتين بناءً على الحد الأقصى لمعامل فقد الحرارة الكلي وأقصى مكاسب حرارية مفيدة. كان الحد الأقصى لمعامل فقد الحرارة الإجمالي لمجمع السربنتين ٥,٥٣ وات/م ٢ ٨.درجة مئوية. أقصى مكاسب حرارية مفيدة لمجمع السربنتين كانت ٥٦١ وات. وجد أن أداء المجمع يزداد مع زيادة الإشعاع الشمسي ومعدل تدفق كتلة الماء ، بينما ينخفض مع ارتفاع سرعة الرياح. بلغت أقصى كفاءة لمجمع السربنتين ٦٦,٦٪ عند معدل تدفق ٠,٠٤٢ كجم / ثانية بينما كانت أقصى زيادة في درجة حرارة خزان الماء في مجمع السربنتين ٢٥,٨ درجة مئوية عند معدل تدفق الكتلة ٠,٠٥ كجم / ثانية

الكلمات المفتاحية: نظام تسخين المياه بالطاقة الشمسية ، مجمع المعوجة ، أنبوب نحاسي ، تسخين المياه ، درجة حرارة التخزين.